

Analysis of Averaged β Value in Two Dimensional Equilibria of a Field-Reversed Configuration with End Mirror Fields

SUZUKI Yukihiisa, OKADA Shigefumi and GOTO Seiichi

Plasma Physics Laboratory, Graduate School of Engineering, Osaka University, Suita 565-0871, Japan

(Received: 8 December 1998 / Accepted: 13 May 1999)

Abstract

Two dimensional (2D) MHD equilibria of a field-reversed configuration (FRC) influenced by the end mirror fields are investigated. 2D numerical equilibrium code incorporating the end mirror effect is used for this study. The results of this calculation indicate that the shape of the axially elongated equilibrium is changed by the end mirrors. Averaged beta $\langle\beta\rangle$ are obtained from these numerical equilibria. The dependence of $\langle\beta\rangle$ on the X_s is compared with Barnes relationship. Here, X_s is the ratio of separatrix to the wall radius. Numerical results for the mirror ratio (R_m) is 1.0 indicates good agreement with Barnes relationship. For the case of $R_m > 1.0$, numerical results come to differ from this relationship. This analysis shows that large R_m makes X_s large and limits the domain of X_s .

Keywords:

FRC, 2D equilibrium, mirror field, averaged beta, Barnes relationship

1. Introduction

An FRC plasma [1] is one of the compact toroid. This plasma has high averaged beta $\langle\beta\rangle$ from 0.5 to 1.0. Here, $\langle\beta\rangle$ is the volume average of β within the separatrix at the mid plane of $z = 0$. Because of such a characteristic, this plasma may be influenced by the change of external magnetic field. The modification of the mirror ratio (R_m) at the end of the FRC is one of the example of this. This mirror effect may give a possibility of equilibrium shape control. As an actual example, the equilibrium of FRC plasma confined within the geometry of FRC Injection Experiment (FIX) machine [2] is thought to be governed by the end mirror fields because of its large mirror ratio from 2 to 6. The equilibrium shape and its characteristics are, then, expected to be clarified with the aid of numerical computation of the FRC equilibrium introducing the mirror field at the end region. Especially, it is important to consider the change of β value corresponding to the change of mirror ratio with numerical computation.

Because the change of β value thought to affect the nature of the stability and the transport. The purpose of this study is to investigate the dependence of $\langle\beta\rangle$ on R_m together with the shape change.

2. 2D Equilibrium Calculation Model

A two dimensional MHD equilibrium code we have developed [3] is used for this study. Because the FRC plasma is axially symmetrical in the cylindrical coordinate system (r, θ, z) , the equilibrium configuration is determined by solving the Grad-Shafranov equation (Eq. (1)) in (r, z) plane.

$$\Delta^* \varphi(r, z) = r \frac{\partial}{\partial r} \left(\frac{1}{r} \frac{\partial \psi}{\partial r} \right) + \frac{\partial^2 \psi}{\partial z^2} = -r^2 \frac{dP(\psi)}{d\psi}, \quad (1)$$

where ψ is the poloidal flux function and $P(\psi)$ is the scalar pressure profile function which depends on the magnetic flux function ψ . In this code, the iterative method to deal with the nonlinear eigenvalue problem

Corresponding author's e-mail: suzuki@ppl.eng.osaka-u.ac.jp

[4] is used to solve Eq. (1).

As $P(\psi)$ the following function is assumed.

$$\frac{dP(\psi)}{d\psi} = \begin{cases} -c(1 + \varepsilon\psi) & (\psi \leq 0) \\ -ce^{-\gamma\psi} & (\psi > 0), \end{cases} \quad (2)$$

Here c is the eigenvalue, ε and γ are profile parameters. In Eq. (2), ψ is negative inside the separatrix and positive outside the separatrix. We can control the separatrix radius by the value of ε [5]. When the value of ε is larger, the separatrix radius become smaller. The separatrix shape can also be changed by γ without mirror effect [6]. A larger value of γ produces a race-track shape equilibrium and a smaller value of γ produces elliptical shape equilibrium.

The boundary condition used in this code is shown in Fig. 1. Here, $\psi = 0$ at $r = 0$ and on the separatrix, $\partial\psi/\partial z = 0$ at $z = 0$ and $z = z_L$ which express that field lines are parallel to z axis. The perfectly conducting wall condition is employed at the wall position as $\psi = \psi_w = 1$, so the flux is conserved within the conducting shell. Therefore, the effect of mirror field can be incorporated with this code by diminishing r_{w2} , that is the wall radius at the mirror position $z \geq z_2$. The calculative domain shown in Fig. 1 contains the taper region which is the area from $z = z_1$ to z_2 . It is difficult to generate rectangle meshes of the equal size in this region. The problem induced from this tapered region is overcome by the grid generation method [7] to be able to optimize meshes in r - z domain.

3. Results

In the first, two types of equilibria are calculated without end mirror effect. The one is calculated with the small gradient of $P(\psi)$ near the separatrix ($\gamma = 25.0$ in Eq. (2)), and the other with the large gradient of $P(\psi)$ (γ

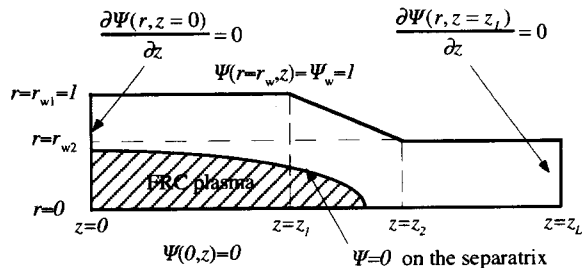


Fig. 1 The boundary condition for the 2D FRC equilibrium with the end mirror field. The perfectly conducting shell is assumed at the wall position. The mirror field is generated when the condition of $r_{w1} > r_{w2}$ is satisfied.

$= 200.0$ in Eq. (2)). These results are shown in Fig. 2(a) ($\gamma = 25.0$) and Fig. 3(a) ($\gamma = 200.0$). In the case of $\gamma = 25.0$, the equilibrium shape is elliptical and in the case of $\gamma = 200.0$, equilibrium shape is race-track. Where elliptical shape equilibrium denotes that the flux function increases gradually from the mid plane ($z = 0$) to the edge of the FRC plasma, and as for the race-track

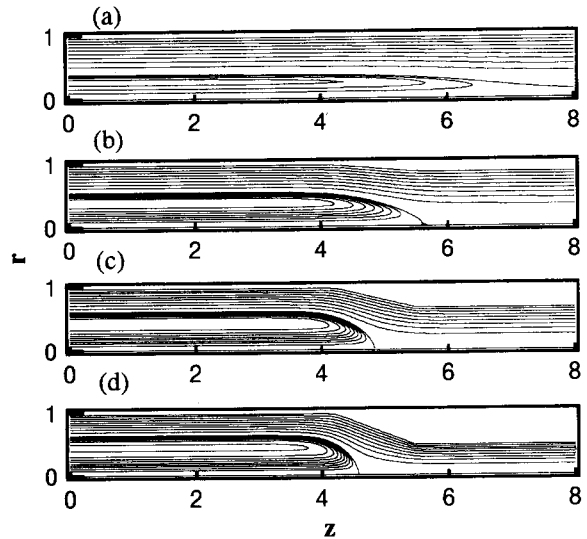


Fig. 2 A series of 2D equilibria for $\gamma = 25.0$ and $\varepsilon = 40.0$ for increasing R_m . The values of R_m are (a) 1.00, (b) 1.23, (c) 2.04, (d) 4.00.

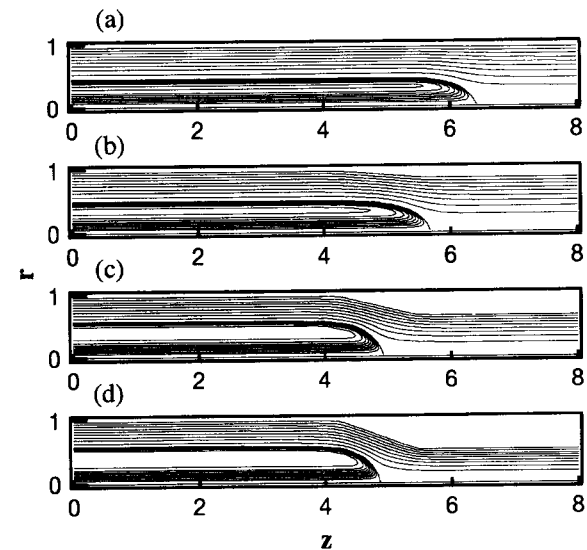


Fig. 3 A series of 2D equilibria for $\gamma = 200.0$ and $\varepsilon = 40.0$ for increasing R_m . The values of R_m are (a) 1.00, (b) 1.23, (c) 2.04, (d) 4.00.

shape equilibrium, the flux fraction increases steeply near the edge of FRC. When $\gamma = 25.0$, the pressure gradient near the separatrix is smaller than the case of $\gamma = 200.0$. Hence the axially distribution of flux surfaces are thought to become gradually in the elliptical case. These two types of equilibria without mirror fields ($R_m = 1.0$) are used for the initial condition to explore the difference of the end mirror effect between two types of equilibria. In this study, thin and long FRC model as observed in the experiment, $X_s = 0.35 \sim 0.45$ and $l_s > 10$, is used for initial condition. Here, l_s shows the separatrix length normalized by the wall radius.

Results of calculations executed against R_m from 1.0 to 4.0 are shown in Fig. 2 and Fig. 3. In these calculations ε is fixed at 40.0. The separatrix shape with the ellipse in the initial (Fig. 2(a)) is changed to the race-track shape (Figs. 2(b),(c),(d)) according to the increase of R_m . This variation occurs in $R_m > 2$. The race-track shape in the original state (Fig. 3(a)) keeps the same independently with R_m (Figs. 3(b),(c),(d)). In the both cases, X_s increased and l_s decreased according to the increase of R_m . Suzuki and Hamada [8] discussed the dependence of X_s on the R_m for the thick FRC equilibrium as $X_s = 0.8 \sim 0.9$. Their results are similar to those of this study in that X_s is saturated when R_m reaches the sufficiently large value. In the case of their results, X_s is saturated for $R_m > 5$. In our results, X_s is saturated for $R_m > 2$. Those difference between the two results may be caused by the difference of X_s .

Averaged beta are calculated by using these solutions of 2D equilibrium. An averaged beta $\langle \beta \rangle$ of the FRC is defined as follows [9].

$$\langle \beta \rangle = \frac{2}{r_s^2} \int_0^{r_s} \beta(r) r dr. \quad (3)$$

Here $\beta(r)$ indicates the radial profile of the beta value. The integral of Eq. (3) is performed within the separatrix at $z = 0$. Figure 4 shows the dependence of $\langle \beta \rangle$ on R_m . In this figure each solid marker is obtained from a numerical 2D equilibrium solution by using Eq. (3). Fig. 4 indicates that in the initially elliptical case for $\gamma = 25.0$, $\langle \beta \rangle$ is changed from 0.95 ($X_s = 0.45$, $l_s = 14.3$, $R_m = 1.0$) to 0.98 ($X_s = 0.63$, $l_s = 9.1$, $R_m = 4.0$). The increment of $\langle \beta \rangle$ is small in this case. In the original race-track case for $\gamma = 200.0$, $\langle \beta \rangle$ is changed from 0.84 ($X_s = 0.45$, $l_s = 12.8$, $R_m = 1.0$) to 0.94 ($X_s = 0.6$, $l_s = 9.3$, $R_m = 4.0$). The increment ratio of $\langle \beta \rangle$ for $\gamma = 200.0$ is larger than for $\gamma = 25.0$. The increment of $\langle \beta \rangle$ is mainly occurred from $R_m = 1.0$ to $R_m = 2.0$. When the R_m increases, l_s decreases as shown Fig. 2 and Fig. 3. If the edge of FRC pushed into the left side from the taper

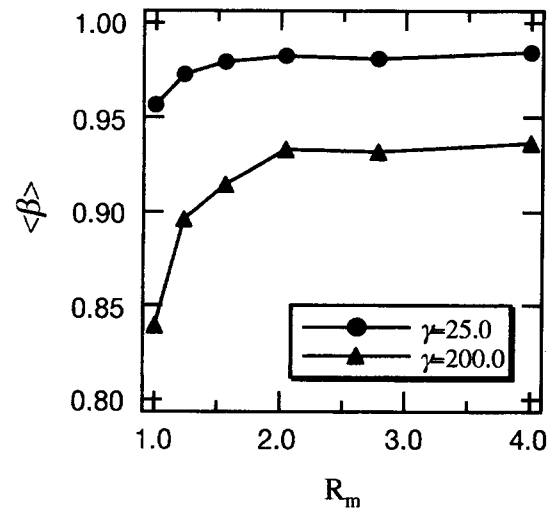


Fig. 4 The average β is displayed as a function of the mirror ratio R_m .

region, the FRC equilibrium is not sufficiently influenced by the change of R_m . It is likely that the saturation of $\langle \beta \rangle$ is caused by the reason described above.

4. Analysis of the Averaged Beta

If the conducting wall is sufficiently longer than the l_s , and there are no plasma pressure outside the separatrix and no end mirror effect, the well known condition derived from axial force balance is satisfied for the FRC [9].

$$\langle \beta \rangle = 1 - \frac{1}{2} X_s^2. \quad (4)$$

Equation (4) called Barnes relationship. In this study, the dependence of $\langle \beta \rangle$ on X_s under the end mirror effect is compared with Barnes relationship. X_s can be varied by changing the value of ε for this calculation. These results are shown in Fig. 5. In this figure, all calculations are performed at $\gamma = 25.0$. When $R_m = 1.0$, the numerical results show the good agreement with Barnes relationship. According to the increase of R_m , the relation between $\langle \beta \rangle$ and X_s of numerical results come to differ from those of Eq. (4). In the case of $R_m = 2.04$, $\langle \beta \rangle$ varies from 0.9 to 0.98 against the small change of X_s . Fig. 5 indicates that a large R_m produces the equilibrium with large X_s and limits the domain of X_s . The mirror fields contribute the magnetic pressure toward the axial direction. As a result, the total magnetic pressure for the axial direction is increased by the mirror field. The integration of plasma pressure inside the separatrix should increase to balance the magnetic

pressure. For those reason, the relation between $\langle\beta\rangle$ and X_s may shift from Barnes relation as shown in Fig. 5.

5. Conclusions

2D numerical equilibria of FRC under the effect of mirror fields are obtained with the boundary condition shown in Fig. 1. In the case of $\gamma = 25.0$ calculations, the equilibrium shape is elliptical at $R_m = 1.0$. According to the increase of R_m , the shape of equilibrium changes to race-track type. On the other hand, when $\gamma = 200.0$, the equilibrium shape is race-track at $R_m = 1.0$ and is kept original state for the condition of $R_m > 1.0$. The dependence of $\langle\beta\rangle$ on R_m is studied. The increase of $\langle\beta\rangle$ is observed when R_m changes from 1.0 to 4.0. The increment ratio of $\langle\beta\rangle$ for $\gamma = 200.0$ is larger than for $\gamma = 25.0$. The increment ratio of $\langle\beta\rangle$ against R_m may depends on the pressure gradient near the separatrix. The dependence of $\langle\beta\rangle$ on X_s under the influence of end mirror field is compared with Barnes relationship. At $R_m = 1.0$, the numerical results indicates good agreement with Barnes relationship. For the condition of $R_m > 1.0$, numerical results are differ from Eq. (4) are shown. So far as this study is concerned, large R_m ($R_m > 2.0$) makes the X_s large and restricts the domain of X_s .

References

- [1] M. Tuszewski, Nucl. Fusion **28**, 2003 (1988).
- [2] H. Himura, S. Okada, S. Sugimoto and S. Goto, Phys. Fluids **28**, 1810 (1995).
- [3] Y. Suzuki, S. Sugimoto, S. Okada and S. Goto, Technol. Repts. of Osaka Univ. **46**, 143 (1996).
- [4] D.W. Hewett and R.L. Spencer, Phys. Fluids **26**, 1299 (1983).
- [5] K. Suzuki and S. Hamada, J. Phys. Soc. Jpn. **55**, 3705 (1986).
- [6] R.L. Spencer and M. Tuszewski, Phys. Fluids **28**, 1810 (1985).
- [7] J.F. Thompson, Z.U.A. Warsi and C.W. Mastin, *Numerical Grid Generation Foundations and Applications* (Elsevier Science Publishing Co., Inc., New York, 1985) p.133.
- [8] K. Suzuki and S. Hamada, J. Phys. Soc. Jpn. **53**, 16 (1984).
- [9] W.T. Armstrong *et al.*, Phys. Fluids **24**, 2068 (1981).

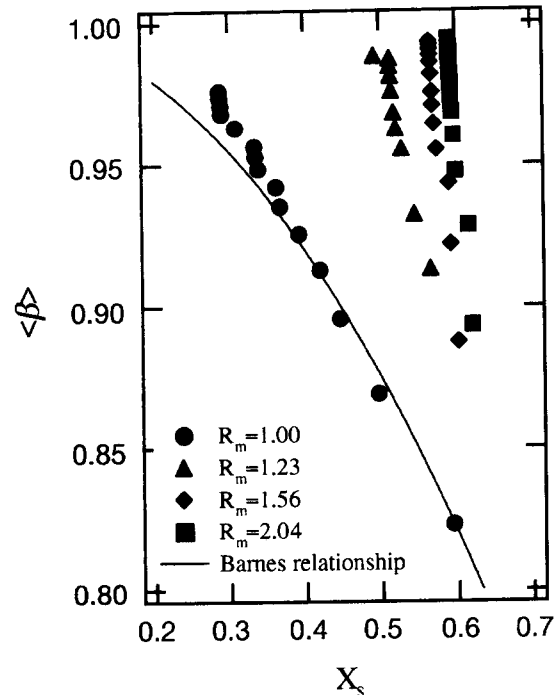


Fig. 5 The average β is displayed as a function of the X_s . The solid line is obtained from Barnes relationship.